COMPARISON OF DRYING KINETICS OF SPENT GRAIN DRIED ON INERT MATERIAL OF DIFFERENT HEAT CAPACITY

Magdalena Zielinska [a,b], Stefan Cenkowski [b]

[a] Department of Agri-Food Process Engineering, University of Warmia and Mazury, Heweliusza 14, 10-718 Olsztyn, Poland

[b]Department of Biosystems Engineering, University of Manitoba, Winnipeg, MB, Canada R3T 5V6

Abstract. *The paper presents the preliminary results of distiller's spent grain (DSG) drying in superheated steam (SS). The objective of this study was to compare the drying kinetics of wheat distiller's spent grains dried on inert material of two different heat capacities. The steam temperatures used were: 110, 130, and 160°C with steam velocities of 0.5, 0.7 and 1 m/s. Drying experiments were conducted under or near to atmospheric pressure (the maximum chamber pressure was approximately 1 kPa above the atmospheric pressure). The approach used to determine the drying kinetics of DSG on the inert material was based on single element drying. The inert material was a sphere composed of Virgin Teflon® PTFE (polytetrafluoroethylene) on which a layer of DSG was deposited and dried in SS. Solid and hollow teflon spheres were used to mimic different heat capacities of the inert material. Experiments involved recording the mass and temperature changes during the course of SS drying.*

Keywords: drying, superheated steam, wheat distiller's spent grain, inert material, heat capacity

INTRODUCTION

Global production of ethanol has been growing around the world in recent years. Decrease in dependency on fossil fuels and increase in demand of ethanol as a fuel additive have led to a dramatic increase in the amount of feedstock used for ethanol production (Keshun, 2008). Currently, almost all ethanol production in Canada is mainly based on renewable agricultural feedstock such as corn and wheat. To reduce the total cost of ethanol production, the remaining material from ethanol distillery, such as distillers' spent grain (DSG) is sold to livestock producers as an excellent source of protein and energy. There are numerous potential markets that can be developed using wheat-based dried distillers' spent grain. Although new food products for human consumption may be derived with time from the ethanol industry, as currently, the only market for wheat-based ethanol co-products are the beef and cattle sectors.

Distillers' spent grain is usually dried to about 10 % w.b. (wet basis) moisture content to lengthen its shelf-life, prolong the storage time and lower the transportation cost (Woods et al., 1994). Superheated steam drying is a drying technology with potential advantages in practise (Tang et. al., 2000). Superheated steam has heat transfer properties superior to air at the same temperature. One of the most obvious advantages of SS is the ability to recover all the latent heat by condensing the exhaust steam. Higher drying rates are possible in both constant and falling rate periods and are dependent on the SS temperature. The higher thermal conductivity and heat capacity of SS lead to higher drying rates for surface moisture above the so-called inversion temperature. In the falling rate period of drying, the higher product temperature in SS leads to a higher value of water diffusivity and a lack of diffusional resistance to water vapour resulting in a faster drying rate (Kudra & Mujumdar, 2002). It is also known that many food products form case-hardening skin in rapid air drying but not in SS. Therefore, more intensive drying conditions can be used. Advantages of this technology are numerous and include: potential in energy recovery from used steam, higher drying rate, drying time reduction, recovery of solvents and volatiles, emission reduction, fire and explosion risk elimination during drying.

Fixed bed, fluidized bed, pneumatic conveying, flash, and impingement SS driers have been used to dehydrate a variety of products on the industrial, pilot, and laboratory stages. A number of food products such as carrots, potatoes, cauliflower, celery, asparagus, leek, wheat, flour, meat, herbs, spices, rice, noodles, brewer's spent grain and distiller's spent grain have been studied and found to be suitable for processing and drying with SS (van Deventer & Heijmans, 2001; Tang & Cenkowski, 2000; Taechapairoj et al., 2006; Markowski, et. al., 2003; Tang et. al., 2005). Although fluidized and spouted bed dryers were originally developed for particular granular and solid materials (i.e., grain, oilseeds and legumes), adding uniformly sized inert particles enables drying of liquid, suspension, slurry, pulp, and paste material (Orsat and Raghavan, 2007). In view of the high moisture content of distiller's spent grain, drying should be performed in different constructions of a fluidized bed of inert particles that provide good conditions for slurry dehydration (Kudra & Mujumdar, 2002). Despite numerous published papers on the subject of drying slurry and paste like material on inert particles, there is insufficient data available in the literature that can be used for modeling of the drying process.

Mathematical modeling and computer simulation of drying processes is one of the most advanced tools in studying various configurations of the process. These models require information about the thermophysical properties of dried material and empirical relationships on material drying characteristics named thin-layer drying equations. The wet solid distributed on the large surface of the inert particles forms a thin layer in which the drying process occurs. The problem with thin layer drying of slurries is that the drying medium can not get through the

slurry, but washes that layer around its developed surface. Also, it is difficult to separate energy that goes to the inert material from energy used in slurry drying on inert material in the form of a thin layer. We believe that the shape and size of the inert material can play a significant role in drying. This is due to the effect of the Nusselt number which controls the heat transfer from SS to material and which depends on the Reynolds number, which in turn depends on the shape and size of the inert particles. A larger mass of inert material requires larger amount of heat to bring that material above the saturation point in SS drying. Normally, the velocity of the drying medium is established arbitrarily by a user-researcher, but that affects the amount of condensation on material surface before it reaches the steam saturation point, which at the end affects total drying time. It is expected that the larger in size of inert material we use, the more condensation will be created on its surface, in turn affecting the drying characteristic.

Therefore, this study has been conducted to provide some experimental results on the effect of different heat capacity of inert particle on the drying characteristic of slurry fraction of grain stillage at a selected range of SS temperatures and velocities.

MATERIAL AND METHODS

Material

Wheat stillage

Whole wheat stillage was obtained in 2008 from a local distillery (Mohawk Canada Limited, a division of Husky Oil Limited, Minnedosa, MB) that predominantly processed wheat into ethanol.

Inert material

The purpose of the inert particles is to develop surface area for a better interaction between SS and DSG, which initially is in the form of slurry. The approach used to determine the drying kinetics of distiller's spent grain (DSG) on the inert material was based on single element drying (Pabis et. al., 1998). Exemplifying, an equivalent particle diameter of 3–6 mm is required to maintain hydrodynamic stability of the conical jet spouted bed dryer (Benali & Amazouz, 2006). However, the size of inert sphere used in our drying experiment, approximately ten times the size used in industry scale, allowed us to determine the kinetics of mass changes of DSG. The sphere was made of polytetrafluoroethylene (Virgin Teflon®, PTFE 860) and served as an inert particle. The experiments carried out to date with glass beads, PVC pellets, spherical resin particles, ceramic balls, silica gel particles and teflon spheres proved that virgin teflon is the most suitable because of no attrition, anti-stick properties, high heat application, and high capacity of heat accumulation (Benali & Amazouz, 2006).

To determine the effect of heat capacity of an inert body on the drying kinetics of DSG, two different teflon spheres (solid and hollow sphere) were prepared for the experiments. The value of heat capacity was proportional to the amount of material in the object. The specific heat of the teflon material was 1400 J/kg K (Dupont, 1999). The solid sphere which served as the inert material consisted 0.1492 kg of pure teflon. The surface area of the solid sphere/wet DSG was approximately 8.1×10^{-3} m^2. The size of the solid teflon sphere was Grade 2 (5.08 cm in diameter), the surface was a polished finish (average roughness ranged from 25-35 μin), and roundness was 0.001 TIR (Applied Plastic Technology Inc., Bristol, RI). Both solid and hollow teflon spheres were of the same dimensions. The only difference between the spheres was the mass of samples used during DSG processing. The hollow sphere consisted of 0.0692 kg of

pure teflon. In order to prepare the hollow sphere, the solid teflon sphere was divided into two hemispheres. Material from the interior was removed leaving a 3.5 mm thick wall. The two hollowed hemispheres were connected with two pins. A three dimensional view of the hollow teflon hemispheres connected by pins and used as inert material in superheated steam processing of DSG is shown in Fig.1. The radius of external surface was 25.4 mm, radius of internal surface was 21.9 mm.

Insert Fig. 1.

Sample preparation

Whole stillage was separated into two fractions: solids (wet distiller's grain, or distiller's spent grain, called DSG) and liquid fraction containing solubles (thin stillage) using a Sorvall General Purpose, RC–3 centrifuge (Thermo Scientific Co., Asheville, NC, USA). The centrifuge operated at a relative centrifugal force of 790 × g, with a 1000 mL sample container rotating at a speed of 2200 rpm, on a radius of 0.146 m for 10 min. After separation, the wet solid fraction (DSG) of the highest density was used in further SS processing. It was bagged, kept in a deep freezer at −15°C and thawed at room temperature when needed. The initial moisture content of the wet DSG fraction was 2.90 ± 0.08 % w.b. Moisture content was calculated according to the air-oven drying method (AACC standards, 2000).

Multilayer drying experiments using a single element as the inert material were conducted in a laboratory-scale unit. The mass of approximately 22.0 ± 0.1 g of wet DSG needed for one drying experiment, equivalent to a 3 mm thin-layer, was applied to the inside surfaces of two hemispherical tea strainers. The radius of the tea strainers was approximately 3 mm greater then the radius of the inert material. To ensure good contact between the surface of inert material and the sample to be dried, the wet DSG layer was compressed over the surface of a teflon sphere, and two hemispherical tea strainers were gently removed, leaving a DSG layer on the surface of inert material. An outside fiberglass mesh cage was used around the sample to prohibit DSG from dripping off the inert teflon sphere. The specific properties of fiberglass (high heat resistance and low hygroscopicity) were taken into consideration when choosing the material. A side view of Teflon sphere covered by DSG material and wrapped with fiberglass mesh cage is shown in Figure 2.

Insert Fig 2.

Experimental equipment, procedure and operating parameters

Experimental set-up was designed and built in the Department of Biosystems Engineering, University of Manitoba and was fully described in our previous study (Zielinska et al., 2009). A single experiment consisted of the following sequence of steps: (1) pre-heating 1 (no steam is running through the system for 0.5 h); (2) pre-heating 2 (SS is brought to the required drying operating temperature for 0.5 h and allowed to pass through the drying chamber); (3) sample loading phase (the system does not allow the steam to flow into the depressurised drying chamber for a few seconds); (4) proper drying phase (the system allows the steam to run through the drying chamber with operating processing parameters adjusted to the corresponding level).

The system was designed with instrumentation to measure operating parameters for SS. These parameters included: temperature, flow rate, pressure of the drying medium, and the history of mass and temperature changes in the sample subjected to SS drying chamber. Mass and temperature changes of DSG dried in SS were measured in separate experiments conducted under the same experimental conditions.

The experiments designed for SS system parameters (namely steam temperature, steam velocity, steam pressure) were conducted at selected processing levels. The steam temperature at the inlet of the drying chamber was controlled at the levels of: 110, 130, and 160°C. The velocity of steam passing through the drying chamber was set at the values of: 0.5, 0.7, and 1.0 m/s. Drying experiments were conducted under or near to atmospheric pressure (the maximum chamber pressure was approximately 1 kPa above atmospheric pressure).

Operating values measured for the SS drying of a DSG layer on solid and hollow teflon sphere are summarized in Table 1.

Insert Table 1

Mass measurement

Changes in moisture content of a sample were calculated based on the measured mass changes which were recorded with an accuracy of 0.001 g using an electronic mass balance (Model TR-403, Denver Instrument Co., Arvada, CO, USA). A digital electronic scale was positioned on the top of the drying chamber, and the inert teflon sphere with the wet DSG layer to be dried was suspended by a string from the scale. The mass changes were recorded every 5 s using the mass balance, which was connected to a computer. The drying was continued until the mass remained constant for 5 min. All samples were dried to the final moisture content of 9.6 ± 1.2 % w.b.

During SS processing of DSG on inert material, the upward flow of superheated steam through the drying chamber created a "lifting force" (i.e. sum of all the forces on a body that force it to move upwards), which affected the real mass-change readings. To compensate for these real losses in mass, separate experiments were performed immediately after each drying test. The compensation tests were conducted with inert teflon sphere. To eliminate the changes in moisture content during the experiment, the surface of the spheres were not covered with a DSG layer. The steam conditions were kept the same as during the appropriate drying test. However, the SS flow in the calibration test was manually controlled to bypass the inner drying chamber for 10 min. The difference between the measured mass readings with and without steam passing through the drying chamber was taken into account during the calculation of the real mass changes during SS drying.

Temperature measurement

The experiments were conducted to measure time history of changes in temperature within the superheated steam drying system and in the DSG sample. The temperatures of the superheated steam and the drying sample were measured continuously using 30-gauge T-type thermocouples, which were connected to a data acquisition system. Temperature changes in the DSG layer were recorded every 5 s using a computer, with an accuracy of 0.1°C. The temperature of the DSG was measured by embedding the thermocouple tip into 1.5 mm the DSG layer. A three dimensional view of the hollow teflon sphere used as the inert material in SS

processing of DSG, with the position of thermocouple inserted into the sample is shown in Fig.1. Steam temperature at various locations in the SS chamber was monitored by several thermocouples within ± 3°C of the desired level. The temperature distribution in the drying chamber varied inconsiderably, within the range of 1 or 2°C.

Under each set of drying conditions, the drying tests were conducted in triplicate. An arithmetic average was then taken for data interpretation.

Flow measurement

The steam flow rate control valve was adjusted to achieve the desired mass flow rate for the appropriate steam velocity of: 0.5, 0.7, and 1.0 m/s with an accuracy of 0.02 m/s (Table. 1).

Steam velocity was calculated on the basis of two different measurements. In the first procedure applied, the steam velocity was calculated based on the volumetric flow rate and cross-sectional area of superheated steam flow running through the drying chamber. Volumetric flow rate of the steam was determined by collecting the condensate exiting the SS drier in a certain time and using the specific volume for the processing temperature inside the drying chamber. The specific volume of SS for selected conditions was calculated from superheated steam tables (Irvine and Liley, 1984).

The results were confirmed with a quick and accurate measurement of the superheated steam flow, which was achieved through a vortex meter. Superheated steam exists in a region where temperature and pressure were independent parameters of drying medium and therefore other instrumentation must accompany the vortex meter to ascertain correct measurement. These individual readings were sent to a flow computer (Compart DXF 351 Flow Computer, Endress Hauser GmbH Co., Weil am Rein, Germany) that amalgamates data to accurately provide a flow measurement for the superheated steam. Then, mass flow rate of steam was determined from the readings displayed by the computer connected to the flow rate meter. The measured mass flow rate of SS was converted to a volumetric flow rate, on the basis of specific volume of SS for the appropriate processing temperature, and the steam velocity was calculated.

Pressure measurement

Adequate monitoring of the pressure in the SS system and drying chamber, by three pressure gauges (two for the superheated steam and one for the process water) was performed. The accuracy of the measurements was approximately ± 0.5 kPa.

RESULTS AND DISCUSSION

SS drying kinetics of thin layer of DSG dried on inert single particle

Typical characteristic of drying DSG in 160°C SS and 1 m/s is shown in Figure 3. The open symbols refer to moisture changes and solid triangles show corresponding material temperature. The dashed horizontal line shows the steam temperature (160°C) used in this experiment.

The DSG sample gained moisture at the beginning of drying due to steam condensation on the material surface. The rapid increase in material temperature was observed until the

temperature of the product attained saturation temperature, which is marked by dotted vertical line 1 (Figure 3). Usually this period lasts several seconds (Pronyk et al., 2004; Markowski et. al., 2003). For SS drying temperatures between 110 and 160°C and SS velocity between 0.5 and 1.0 m/s, the warm-up period was between 0.5 and 7.5 min. Due to large surface area of material to be dried, the warm-up period observed during our experiments was longer in comparison to the data reported in the literature (Tang et al., 2005; Pronyk et al., 2004, Markowski et. al., 2003.

Insert Fig. 3.

First drying rate period occurred past the saturation point, when the moisture gained on the surface of the material due to steam condensation (acting as free water) evaporated under 100°C. During this period, the heat transferred to the material was used only to evaporate the free water that condensed on the material surface. The material temperature remained constant until free water disappeared from material surface. It is reasonable to assume that the end of 1st drying rate period occurs when the temperature of material starts to increase. Vertical dotted line 2 (Figure 3) marks the end of that period. In the range of SS temperature and velocity defined in our study, the period associated with the evaporation of the condensate from the surface of a sample was from 7.5 to 35 min. After this time, moisture content of the sample attained its initial value that is marked by horizontal dotted line 3 (Figure 3).

During the next phase of steam drying (period between vertical dotted lines 2 and 4), a very slow and steady increase in material temperature was observed. This is when moisture present in DSG sample began to evaporate. In our experiments the observed increase in material temperature was in the range of 1-5°C. This period could also be included into the constant drying rate until the considerable slope of material temperature was observed. Vertical dotted line 4 (Figure 3) marks this considerable increase in temperature of the DSG sample. In our experiments, the time corresponding to this drying rate period lasted from 35 to 150 min, depending on SS drying conditions. The typical creeping in sample temperature (1-5°C), i.e. period between lines 2 and 4, could be caused by steady shrinking of DSG hindering the movement of moisture to the surface of the dried layer.

Past the dotted line (4), we observed typical 2nd drying rate period where the temperature of DSG began increasing while moisture changes were following an exponential curve and eventually reaching a plateau.

Effect of different heat capacity of inert material on moisture changes in DSG sample

Changes in moisture content of DSG during SS drying on hollow and solid teflon spheres for SS temperature of 110, 130, 160°C and steam velocity of 1.0 m/s are shown in Figure 4 and 5, respectively. All samples had the same initial moisture content of approximately 2.90 ± 0.08% d.b.). Generally, except for the initial stage, the drying rate (slope) appeared to be the same for the thin layer of DSG dried on hollow and solid teflon spheres, at the same SS drying conditions. During the first several minutes to SS exposure, the average water content increased with time in both samples dried on hollow and solid sphere. This was a result of condensation onto the sample surface. However, DSG layer dried on the solid teflon sphere gained more moisture in comparison to DSG sample dried on a hollow sphere. The inserts in Figure 4 and 5 show the enlarged initial period of processing in SS.

Insert Fig. 4.

For example, when material was dried at steam temperature of 160°C and steam velocity of 1 m/s and the steam condensation occurred on the surface of DSG material, the moisture of material distributed on solid sphere increased from its original value of 2.90 up to 3.38 kg water /kg d.b. vs. 3.12 kg water /kg d.b. for material dried on the hollow sphere (Figure 4 and 5). At the range of the SS temperature from 110 to 160°C and the SS velocity between 0.5 and 1.0 m/s, drying on a solid sphere caused the initial moisture content of the sample to increase to the values approximately 10% higher in comparison to the moisture gain on the DSG surface dried on hollow sphere.

Insert Fig. 5.

Effect of SS temperature on moisture changes in DSG sample

SS drying temperature had an important effect on moisture changes in DSG samples. The amount of steam condensed on DSG layer dried on both hollow and solid spheres increased with decreasing the SS temperature. For example, the moisture of material dried on the surface of the hollow sphere at 110°C increased from its original value of 2.90 to 3.54 kg water /kg d.b. in comparison to the increase from 2.90 to 3.12 kg water /kg d.b. for DSG dried at 160°C. However, the maximum moisture of material dried on the surface of the solid sphere at 110°C was 3.81 kg water /kg d.b. vs. 3.38 kg water /kg d.b. for material dried at 160°C (Figure 4 and 5).

It means that the increase in SS temperature from 110 to 160°C caused the initial moisture gain to decrease by approximately 15% for both hollow and solid sphere. The effect of steam temperature on the amount of the moisture gain could be explained by the fact that a certain amount of sensible heat is needed to bring a sample above the saturation point in SS drying (100°C). When the temperature of steam decreased, the sensible heat of the steam decreased as well. Therefore, increased steam condensation took place to provide the required heat for heating up the DSG sample to the saturation point in SS drying.

Effect of SS velocity on moisture changes in DSG sample

Figure 6 shows the changes in moisture of the DSG samples dried on the hollow sphere with respect to SS velocity and their drying time. The experiment was conducted at 160°C and at three steam velocities, namely 0.5, 0.7 and 1.0 m/s. The effect of the velocity of SS is particularly visible during the initial stage of SS drying. For example, the moisture of the material processed at the velocity of 1 m/s increased from its original value up to 3.12 kg water /kg d.b. vs. 3.49 kg water /kg d.b. when steam temperature of 0.5 m/s was used. It means that, the increase in SS velocity from 0.5 to 1.0 m/s during the drying of DSG on the hollow sphere at 160°C caused the initial moisture gain to decrease by 12 % (Figure 6). For all operating conditions studied, it caused the initial moisture gain to decrease by 10-15%.

Insert Fig. 6.

The higher the steam velocity, the smaller the steam condensation on the surface of the DSG material deposited on the hollow and solid sphere was observed. Less heat was transferred from lower SS velocity to the DSG sample by convection because of the lower heat-transfer coefficient between the steam and the sample. Therefore, more condensation on DSG surface was observed before this process was reversed into drying. Furthermore, all three SS velocities gave similar drying rates, except for the small discrepancies observed at the end of drying.

Effect of different heat capacity of inert material on drying time

The warm-up period of the DSG was influenced by the different heat capacity of inert material and was in the range from 0.5 to 2.5 min for the hollow sphere and from 1 to 7.5 min for the solid sphere. Drying of DSG on the hollow sphere caused the warm-up period shorten by 50-67% in comparison to drying of DSG on the solid sphere, for the SS conditions tested in our study. The larger mass of the inert material was used the higher amount of heat was needed to bring the material above the saturation point in SS drying. Also, the different heat capacity of the inert material had a substantial effect on the time duration when the moisture content of the sample regained its initial value (inserts in Figure 4 and 5). Depending on SS drying conditions (in our case temperatures between 110 and 160°C and SS velocity between 0.5 and 1.0 m/s), the 1st drying rate period associated with the evaporation of the condensate from the surface of a sample was from 2.5 to 40 min for the hollow sphere vs. 7.5 to 50 min for the solid sphere. The smaller the heat capacity was used the shorter the drying time to regain the initial moisture content by the material was noted. The higher the steam temperature, the more visible differences in drying time were observed for both cases (hollow and solid sphere). Depending on the SS temperature, drying on the hollow sphere cut this period by 19-60% in comparison to drying of DSG on the solid sphere. A substantial effect of a different heat capacity of inert material on the entire drying time was observed. For example, drying of DSG at 160°C and 1.0 m/s, on the hollow sphere in comparison to drying on the solid sphere cut the entire drying time by approximately 30%.

Effect of SS temperature on drying time

At 160°C and 1.0 m/s the drying of DSG on the hollow sphere in comparison to drying on the solid sphere cut the entire drying time by approximately 30%. However, almost no differences were observable for the lowest SS temperature of 110°C (Figure 4 and 5). Then, the increase in steam temperature from 110 to 160°C had a substantial effect on the entire drying time and caused it to decrease by 77% for the hollow sphere and 68% for the solid sphere, depending on the operating conditions. The increase in steam velocity from 0.5 m/s to 1 m/s resulted in substantial shortening the entire drying time (38%).

Effect of SS velocity on drying time

The higher the SS velocity was used, the shorter the period required to evaporate free moisture was observed. It is in agreement with the data reported by other researchers (Pronyk, 2007). Increasing the steam velocity while keeping the same SS temperature results in faster drying time. In Figure 6, one can observe that the increase in steam velocity from 0.5 m/s to 1.0 m/s resulted in substantial shortening drying time (38%).

Effect of different heat capacity of inert material on temperature changes in DSG sample

The changes in temperature of DSG samples dried on different inert materials (hollow and solid teflon sphere) are shown in Figure 7. The horizontal dashed line refers to the SS temperature in the drying chamber. Drying at SS temperature of 160°C and velocity of 1 m/s was chosen to show representative trend line for temperature changes in DSG layer during the course of drying (Figure 7). The material dried on the solid teflon sphere showed a substantial delay on the temperature rate increases in the 2nd rate period.

Insert Fig. 7.

In the final stage of SS drying, the temperature of DSG layer on the hollow inert sphere attained higher values faster than the temperature of the material deposited on the solid sphere. This can be explained by the fact that a portion of heat is absorbed by the larger mass of the solid inert material. For example, the time for DSG to reach SS temperature of 160°C ranged from 59 to 61 min for the thin layer of DSG placed on the hollow sphere and from 80 to 82 min when the same thickness of DSG layer was deposited on the solid inert sphere. In all cases, the drying time was much shorter (26%) when SS drying of DSG on the hollow teflon sphere vs. SS drying of DSG on the solid teflon sphere.

Effect of SS temperature on the temperature changes in DSG sample

Typical temperature changes in DSG layer during drying on the solid teflon sphere (SS temperature: 110, 130, 160°C; steam velocity: 1 m/s) are shown in Figure 8. A substantial effect of SS temperature on the changes in temperature of DSG layer was noted during warm-up, 1st and 2nd drying rate period. The higher the temperature of SS, the sharper the increase of material temperature was observed at the 2nd drying rate period, and then the shorter time was noted to attain the temperature of SS (Figure 8).

Insert Fig. 8.

Effect of SS velocity on temperature changes in DSG sample

Not only the temperature, but also the velocity influenced the changes in material temperature. Figure 9 shows changes in material temperature during drying of DSG on the solid teflon sphere. The experiments were performed at the SS temperature of 160°C for three steam velocities of 0.5, 0.7, 1 m/s.

Insert Fig. 9.

The SS velocity had an effect on material's temperature only in the 2nd rate period. The higher the SS velocity, the sooner the increase in the temperature of DSG would start climbing, and then the shorter time to attain the SS temperature was noted (Figure 9). It can be explained by the fact that lower range of SS velocity caused higher moisture concentration on DSG surface in comparison to higher range of SS velocity.

CONCLUSIONS

The constant rate drying period and the falling drying rate period were noticeable for the SS drying of a thin layer of a slurry fraction of spent grain on single inert material in the SS temperature ranged from 110 to 160°C and SS velocity between 0.5 and 1.0 m/s. Very slow and steady increase in material temperature was observed at the beginning of 2nd drying rate period when moisture present in DSG sample started to evaporate. The typical creeping in sample's temperature (1-5°C), could be caused by steady shrinking of DSG hindering the movement of moisture to the surface of the dried layer.

Generally, except for the initial stage, the drying rate (slope) appeared to be the same for the thin layer of DSG dried on the hollow and solid teflon spheres, at operating conditions studied. Drying on a solid sphere caused the initial moisture content of the sample to increase to the values approximately 10% higher in comparison to the moisture gain on the DSG surface dried on a hollow sphere. The increase in SS temperature from 110 to 160°C caused the initial moisture gain to decrease by 15% for both the hollow and the solid sphere. The increase in SS velocity from 0.5 to 1.0 m/s during drying of the DSG caused the initial moisture gain to decrease by 10-15% for all operating conditions studied.

The warm-up period of the DSG was influenced by the different heat capacity of inert material and was in the range from 0.5 to 2.5 min for the hollow sphere and from 1 to 7.5 min for the solid sphere.

Drying of the DSG at the highest SS temperature of 160°C (SS velocity 1.0 m/s) on a hollow sphere in comparison to the drying on a solid sphere cut the entire drying time by approximately 30%. However, almost no differences in drying time were observable for the lowest SS temperature of 110°C (SS velocity 1.0 m/s). The increase in steam velocity from 0.5 m/s to 1.0 m/s resulted in substantial shortening the entire drying time (38%).

The material dried on the solid teflon sphere showed a substantial delay on the temperature rate increases in the 2nd rate period in comparison with drying on the hollow sphere.

ACKNOWLEDGMENT

REFERENCES

AACC. Air-Oven Method, Drying at 135°C. In: *Approved Methods of the American Association of Cereal Chemists.* AACC, St. Paul, MN., 2000.

Benali, M. 2004. Thermal drying of foods: Loss of nutritive content and spoilage issues. In A. S. Mujumdar (Eds.), *Drying of products of biological origin.* India: Oxford IBH and Science Publishers.

Benali, M., and M. Amazouz. 2006. Drying of vegetable starch solutions on inert particles: Quality and energy aspects. *Journal of Food Engineering* 74, 484–489.

Caixeta, A.T., R. Moreira, M.E. Castell-Perez. 2002. Impingement drying of potato chips. *Journal of Food Process Engineering* 25, 63–90.

Deventer, H.C. and R.M.H. van Heijmans. 2001. Drying with superheated steam. *Drying Technology* 19 (8), 2033–2045.

DuPont, 1999. Teflon PTFE 850-A: Fluoropolymer Resin. Product Information, DuPont Fluoroproducts << http://www2.dupont.com>>

Gervais, M., C. Pronyk, J. Bunn, and S. Cenkowski. 2004. Design and performance of a laboratory scale superheated steam processing system. *North Central ASAE/CSAE Conference*, Winnipeg, MB.

Irvine, Jr., T.F., and P.E. Liley. 1984. Steam and gas tables with computer equations. Orlando, FL: Academic Press Inc.

Jensen, A.S. 1992. Pressurized drying in a fluid bed with steam. In *Drying' 92*; Mujumdar, A.S., Ed.; Hemisphere Publishing Corporation: New York, 1953–1601.

Keshun, L. 2008. Particle size distribution of distillers dried grains with solubles (DDGS) and relationships to compositional and color properties. *Bioresource Technology* 99, 8421–8428.

Kim, Y., N.S. Mosier, R. Hendrickson, T. Ezeji, H. Blaschek, B. Dien, M. Cotta, B. Dale, and M.R. Ladisch. 2008. Composition of corn dry-grind ethanol by-products: DDGS, wet cake, and thin stillage. *Bioresource Technology* 99, 5165–5176.

Kondjoyan, A. and S.Portanguen. 2008. Prediction of surface and ''under surface'' temperatures on poultry muscles and poultry skins subjected to jets of superheated steam. *Food Research International* 41, 16–30.

Kudra, T., and A. S. Mujumdar. 2002. Advanced drying technologies. NY: Marcel Dekker Inc.

Markowski, M., S. Cenkowski, D.W. Hatcher, J.E. Dexter and N.N. Edwards, 2003. The effect of superheated-steam dehydration kinetics on textural properties of Asian noodles. *Transactions of the ASAE* 46(2), 389–395.

McAloon, A., F. Tayor, W. Yee, K. Ibsen and R. Wooley. 2000. Determining the cost of producing ethanol from corn starch and lignocellulosic feedstocks. NREL/TP-580-28893.

Moreira, R.G., M.E. Castell-Perez, M.A. Barrufet. 1999. Deep-Fat Frying; Aspen Publishers, Inc.: Gaithersburg, Maryland, 275–313.

Nimmol, C., S. Devahastin, T. Swasdisevi, S. Soponronnarit. 2007. Drying of banana slices using combined low-pressure superheated steam and far-infrared radiation. *Journal of Food Engineering* 81, 624–633.

Orsat, V. and G.S.V. Raghavan. 2007. Dehydration technologies to retain bioactive components. In *Functional Food Ingredients and Nutrauceticals: Processing Technologies*, ed. J. Shi, 173-191. Boca raton, FL: CRC/Taylor & Francis.

Pabis, S., D.S. Jayas, S. Cenkowski. 1998. Grain Drying: Theory and Practice. New York, NY: John Wiley & Sons, Inc.

Prachayawarakorn, S., S. Soponronnarit, S. Wetchacama, D. Jaisut. 2002. Desorption isotherms and drying characteristics of shrimp in superheated steam and hot air. *Drying Technology* 20 (3), 669–684.

Pronyk, C. 2007. Effects of superheated steam processing on the drying kinetics and textural properties of instant asian noodles. Unpublished PhD thesis. Department of Biosystems Engineering, University of Manitoba, Canada.

Pronyk, C., S. Cenkowski and W.E. Muir. 2004. Drying foodstuffs with superheated steam. *Drying Technology* 22, 899–916.

Ranken, M.D., C. Baker, R.C. Kill. 1997. Food industries manual. Ed.: London; Melbourne: Blackie Academic & Professional.

Tang, Z., S. Cenkowski. 2000. Comparison of the dehydration dynamics of potatoes in superheated steam and hot air. *Canadian Agricultural Engineering* 42(1), 43–49.

Tang, Z., S. Cenkowski, M. Izydorczyk. 2005. Thin-layer drying of spent grains in superheated steam. *Journal of Food Engineering* 67, 457–465.

Tang, Z., S. Cenkowski and W.E. Muir. 2000. Dehydration of sugar-beet pulp in superheated steam and hot air. *Transaction of the ASAE* 43(3):685-689.

van Deventer, H.C. and R.M.H. Heijmans. 2001. Drying with superheated steam. *Drying Technology* 19(8), 2033–2045.

Woods, B., H. Husain, A.S. Mujumdar. 1994. Techno-economic assessment of potential superheated steam drying applications in Canada. Report 9138 U 888. Canadian Electrical Association, Montreal, QC.

Zielinska, M., S. Cenkowski, M. Markowski. 2009. Superheated steam drying of distillers' spent grains on inert material. *Drying Technology* (In press, 2009).

FIGURE CAPTIONS

Fig. 1. Three dimensional view of a hollow teflon sphere used as inert material in SS processing of DSG. T_1 is temperature of DSG layer measured by T-type thermocouple.

Fig. 2. A single inert element covered by DSG material and wrapped with fiberglass mesh cage – side view.

Fig. 3. Changes in moisture content and material temperature during DSG drying on a solid teflon sphere in SS at 160°C temperature and 1 m/s velocity. Horizontal dashed line indicates SS of temperature 160°. Number (1), (2), and (4) mark specific drying zones, number (3) marks the initial moisture.

Fig. 4. Moisture changes in DSG during drying on a hollow teflon sphere used as inert material (SS temperature: 110, 130, 160°C; steam velocity: 1 m/s). The insert shows the enlarged initial stage of processing in SS.

Fig. 5. Moisture changes in DSG during drying on a solid teflon sphere used as inert material (SS temperature: 110, 130, 160°C; steam velocity: 1 m/s). The insert shows the enlarged initial stage of processing in SS.

Fig. 6. The effect of steam velocity (0.5, 0.7 and 1 m/s) on moisture changes in DSG layer dried on a hollow teflon sphere at 160°C temperature.

Fig. 7. The effect of heat capacity of inert material on temperature changes in DSG dried in SS at 160°C steam temperature and 1 m/s velocity. Horizontal dashed line indicates steam temperature.

Fig. 8. The effect of SS temperature (110, 130 and 160°C) on temperature history of DSG layer dried on a solid inert sphere at one SS temperature of 1 m/s. Horizontal dashed line indicates steam temperature.
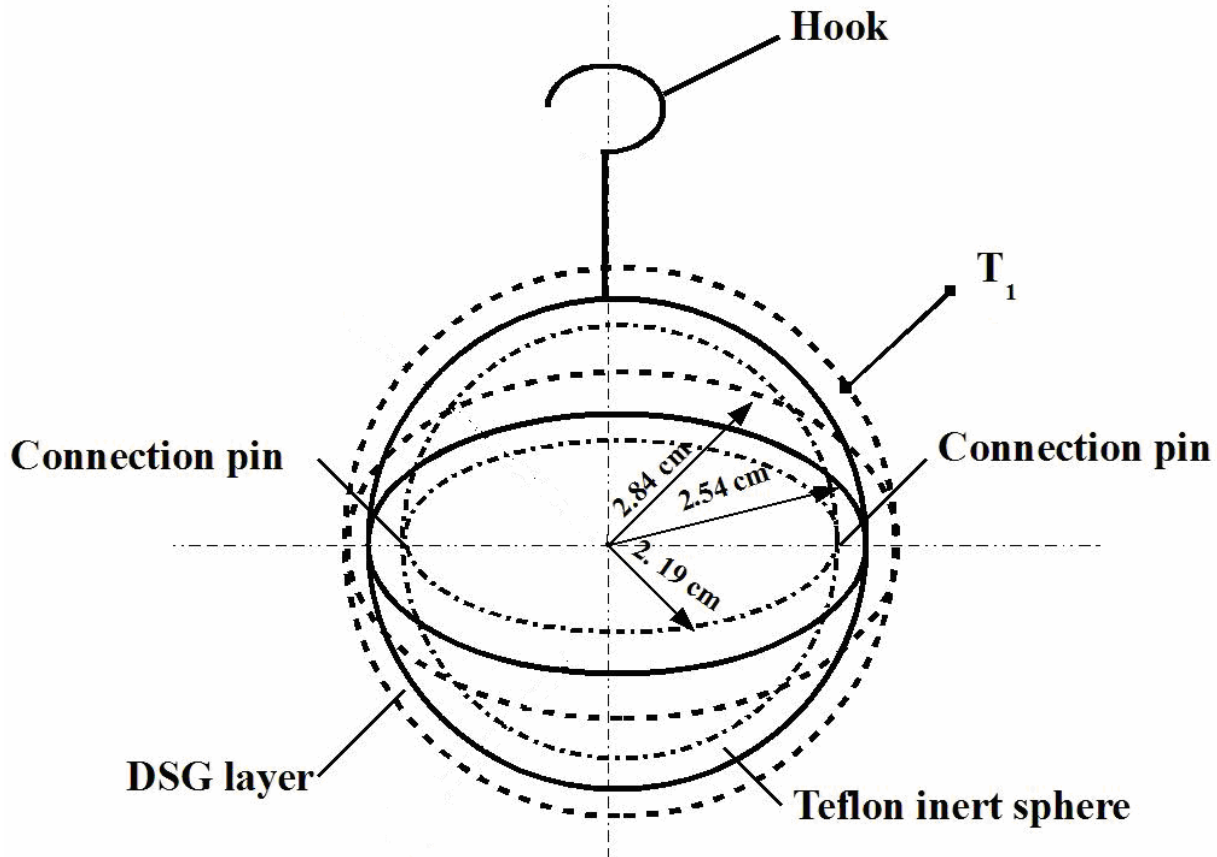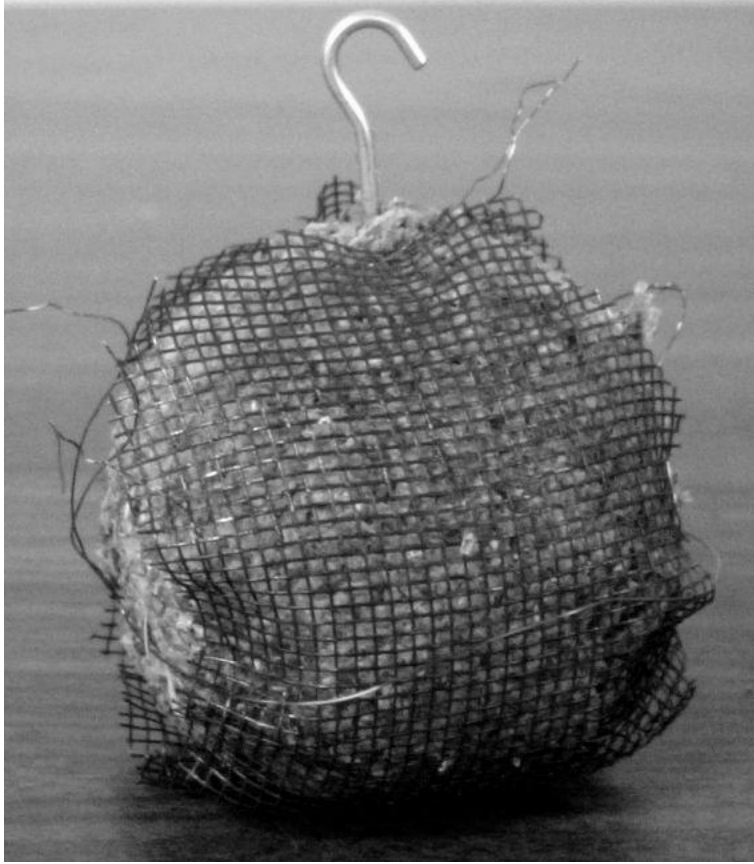
Fig. 9. The effect of steam velocity (0.5, 0.7, and 1 m/s) on temperature changes in DSG layer dried on a solid inert sphere in SS at 160°C temperature. Horizontal dashed line indicates steam temperature.
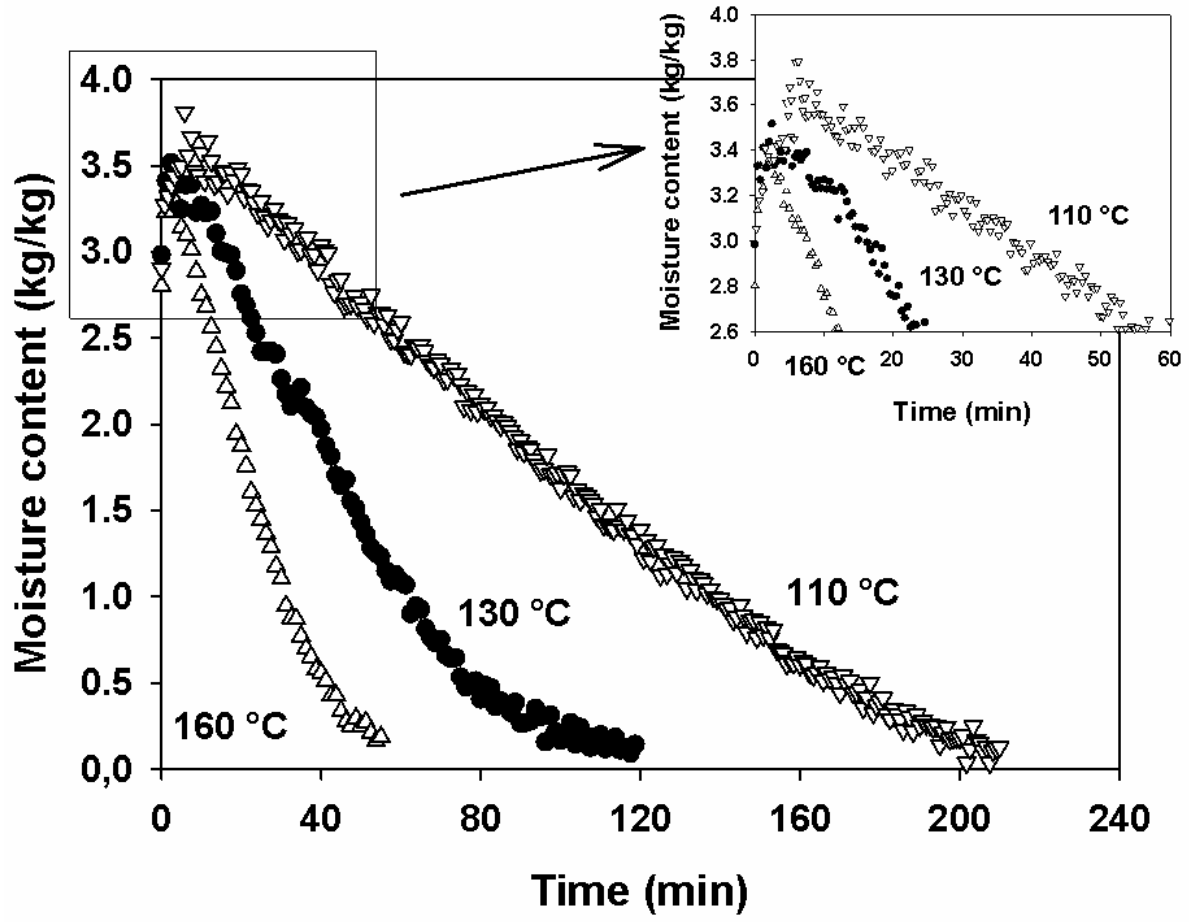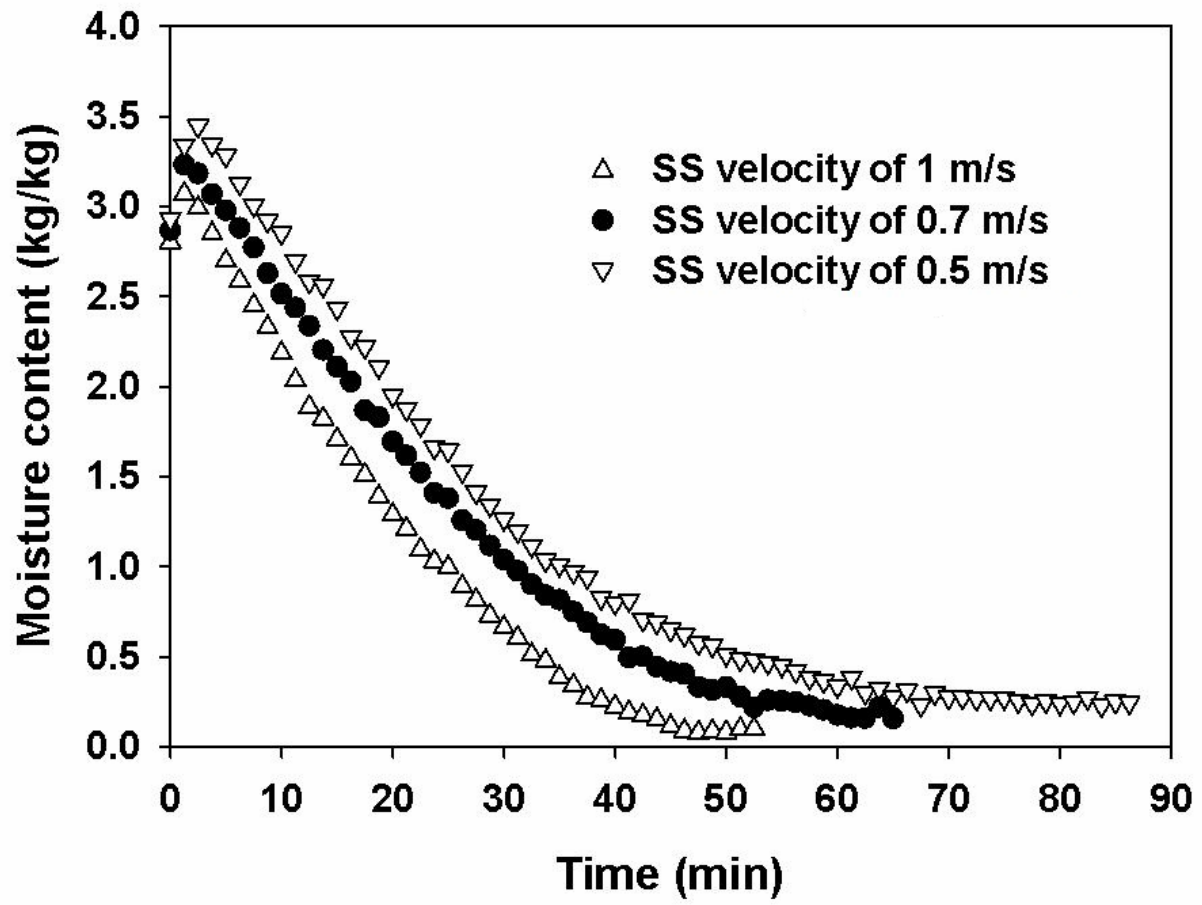

Fig. 1.
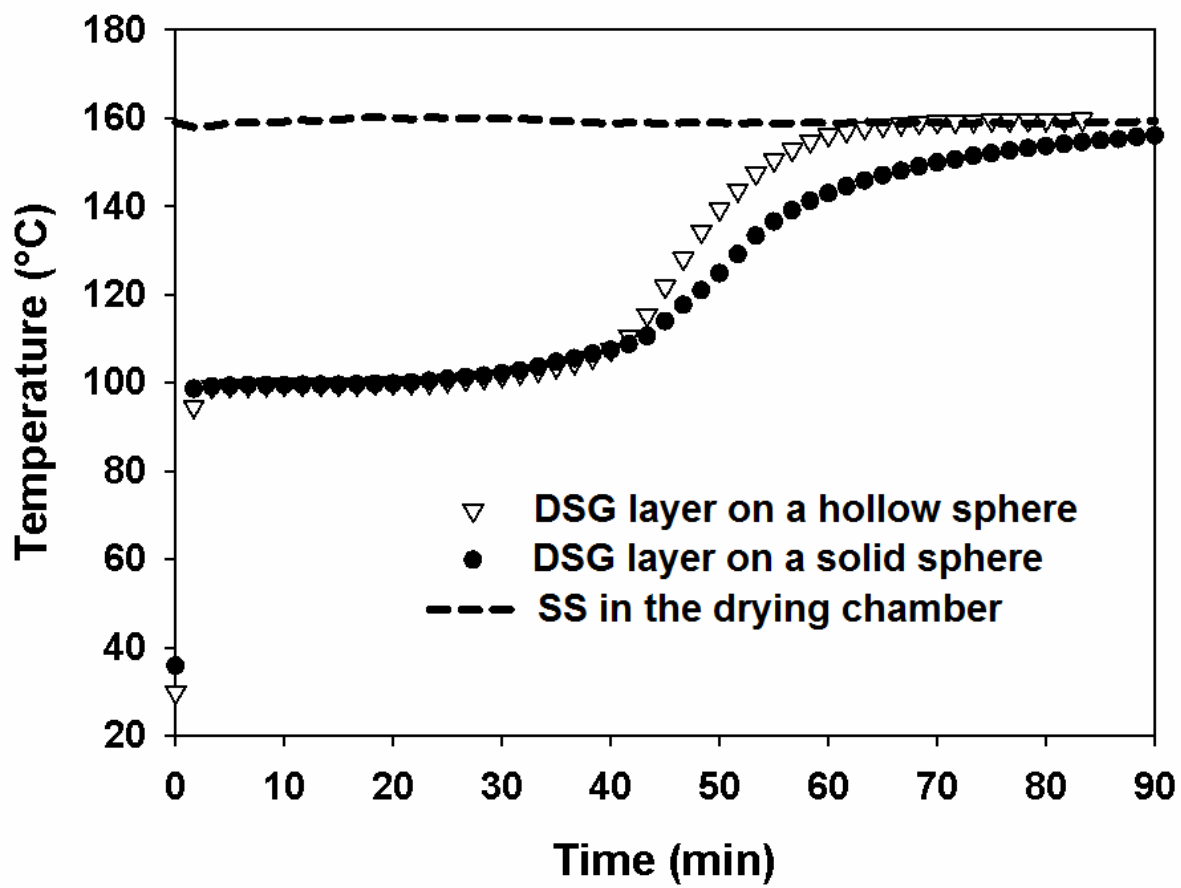
Fig. 2.
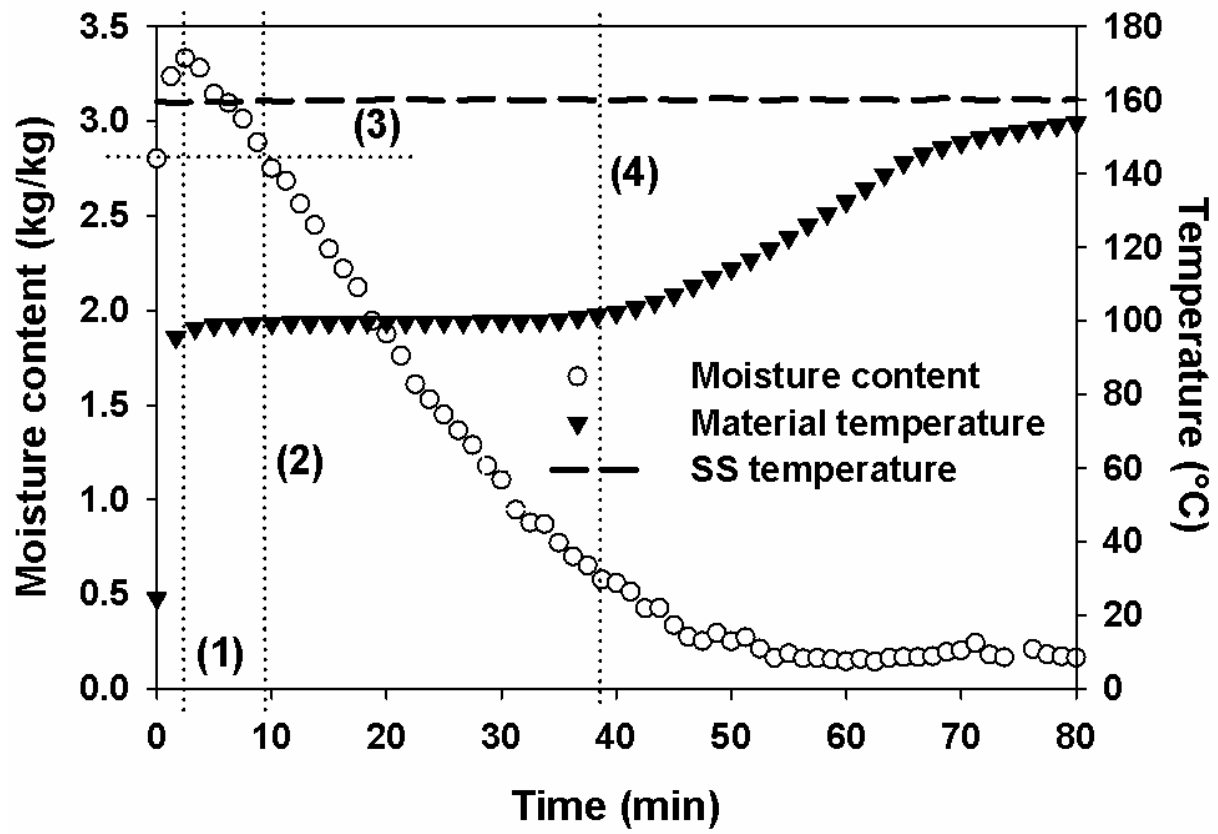
Fig. 3.
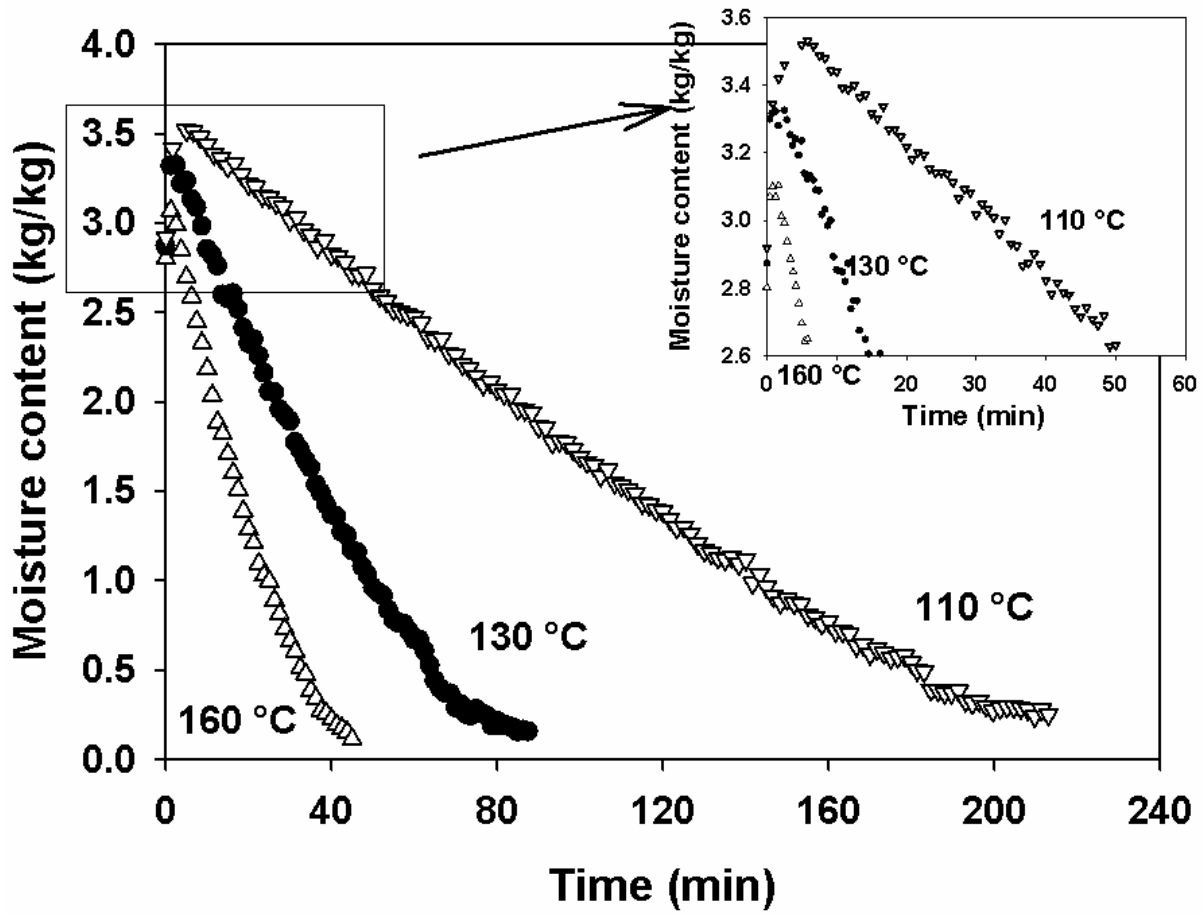
Fig. 4.

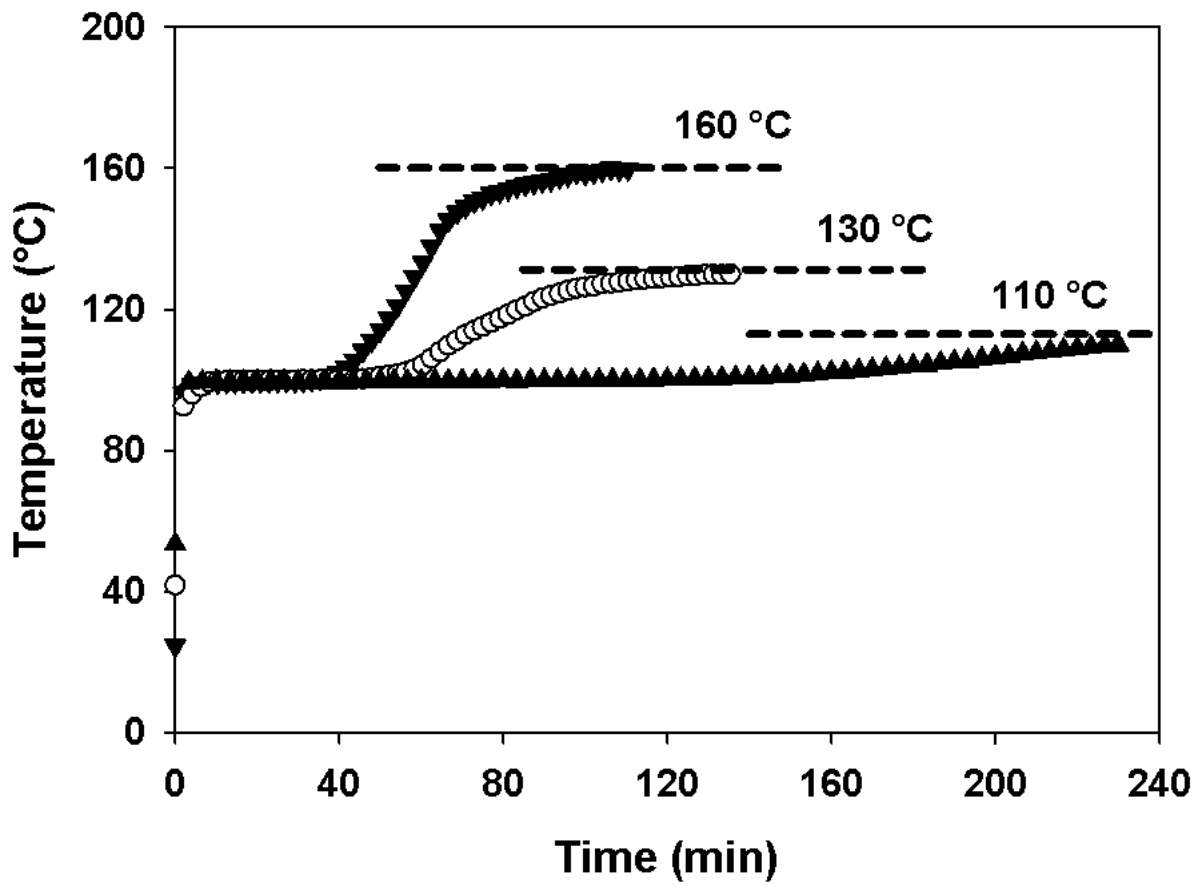Fig. 5.
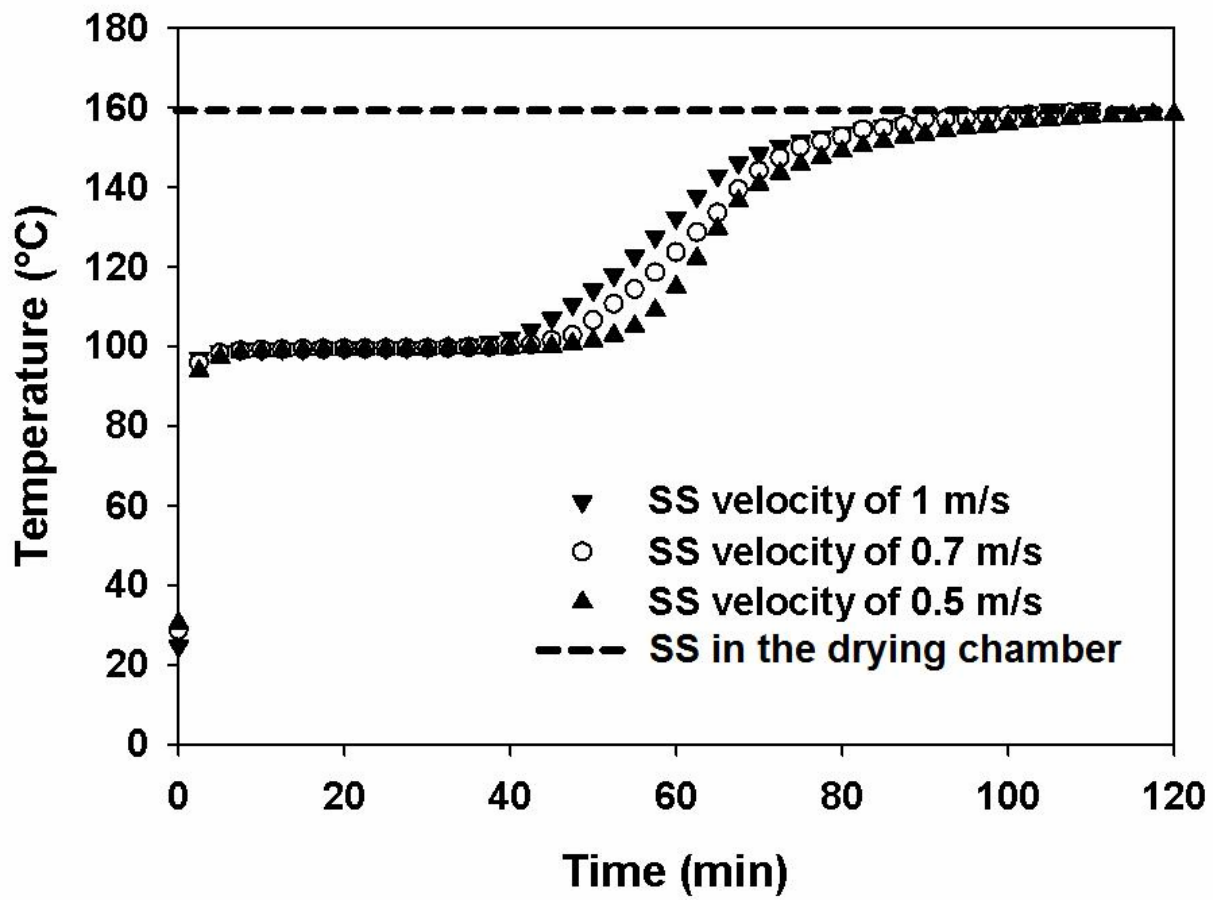
Fig. 6.

Fig. 7.

Fig. 8.

Fig. 9.

Table 1. Operating values measured for the SS drying of DSG on solid and hollow teflon sphere.

Inert Material	SS Temp. (°C)	SS Velocity (m/s)	SS Pressure (kPa)	Specific volume (m^3/kg)	Volume of condensate (m^3/h) ×10^{-3}	Superheater Temp. (°C)
	110	0.49	0	1.72165	6.48	182
	110	0.71	0.5	1.71307	9.12	154
	110	0.99	1	1.70458	12.96	143
	130	0.50	0	1.81676	6.12	232
Solid	130	0.72	0.5	1.80774	8.88	193
	130	0.97	1	1.79881	12.12	171
	160	0.49	0	1.95770	5.64	326
	160	0.70	0.5	1.94801	8.04	243
	160	1.00	1	1.93842	11.52	232
	110	0.51	0	1.72165	6.60	182
	110	0.71	0.5	1.71307	9.24	154
	110	0.99	1	1.70458	12.60	143
	130	0.50	0	1.81676	6.18	232
Hollow	130	0.71	0.5	1.80774	8.76	193
	130	1.01	1	1.79881	12.60	176
	160	0.49	0	1.95770	5.58	315
	160	0.69	0.5	1.94801	7.92	249
	160	0.98	1	1.93842	11.34	226